# Violation of Bell's Inequality and Classical Probability in a Two-Photon Correlation Experiment

Z. Y. Ou and L. Mandel

*Department of Physics and Astronomy, University of Rochester, Rochester, New York 14627*

(Received 22 February 1988)

Correlation measurements of mixed signal and idler photons produced in the process of parametric down-conversion have been performed as a function of two linear polarizer settings. It is found that the Bell inequality for two separated particles is violated by about 6 standard deviations, and that classical probability for light waves is violated substantially also.

PACS numbers: 42.50.Wm, 42.50.Dv

Although the quantum-mechanical paradox relating to Einstein locality has now been investigated in several optical correlation experiments,[1-9] some of which exhibited an explicit violation of Bell's inequality,[3,5-9] there still appears to be interest in new observations of this type. In the most successful of the past experiments the two correlated photons were produced in the cascade decay of calcium atoms.[6,7] More recently several observations of nonlocal quantum correlations were reported in experiments in which the correlated particles were derived from the interference of signal and idler photons created in the process of parametric down-conversion.[9-11]

In the following we report another photon correlation experiment of this type, similar to one first performed by Alley and Shih,[9] in which the observed violation of Bell's inequality for two separated particles is as large as 6 standard deviations. At the same time we also show that classical probability relating to the wave properties of light is violated to a significant extent in this correlation experiment.

An outline of the experiment is shown in Fig. 1. Light from the 351.1-mm line of an argon-ion laser falls on a nonlinear crystal of potassium dihydrogen phosphate, where down-converted photons of wavelength about 702 nm are produced. When the condition for degenerate phase matching is satisfied, down-converted, linearly polarized signal and idler photons emerge at angles of about $\pm 2°$ relative to the uv pump beam with the electric vectors in the plane of the diagram. The idler photons pass through a 90° polarization rotator, while the signal photons traverse a compensating glass plate $C_1$ producing equal time delay. Signal and idler photons are then directed from opposite sides towards a beam splitter (BS), as shown. The light beams emerging from the beam splitter, consisting of mixed signal and idler photons, pass through linear polarizers set at adjustable angles $\theta_1$ and $\theta_2$, and through similar interference filters (IF), and finally fall on two photodetectors $D_1$ and $D_2$. The photoelectric pulses from the two detectors, after amplification and pulse shaping, are fed to the start and stop inputs of a time-to-digital converter (TDC) under computer control, that functions as a coincidence counter. The coincidence counting rate, after subtraction of accidentals, provides a measure of the joint probability $P(\theta_1,\theta_2)$ of detecting two photons for various setting $\theta_1,\theta_2$ of the two linear polarizers.

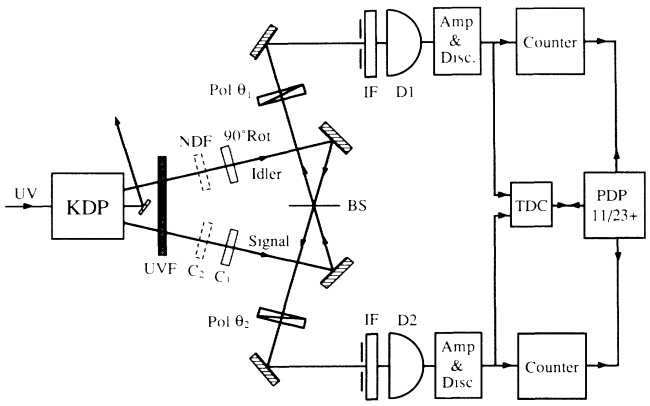


FIG. 1. Outline of the apparatus.

The usual locality argument, with the assumption that any two-particle correlations are attributable to some hidden variable, with the no-enhancement hypothesis of Clauser and Horne,[12] and with the assumption that the detectors do not depend on the hidden variables, leads to the well-known Bell inequality[12-14]

$$S = P(\theta_1,\theta_2) - P(\theta_1,\theta_2') + P(\theta_1',\theta_2') + P(\theta_1',\theta_2) - P(\theta_1',-) - P(-,\theta_2) \le 0. \quad (1)$$

$P(\theta_1',-)$ and $P(-,\theta_2)$ are the corresponding probabilities with one or the other linear polarizer removed. We now calculate the joint probability $P(\theta_1,\theta_2)$ first by quantum mechanics and then by classical wave optics.

*Quantum theory.*—If the input to the dielectric beam splitter BS consists of an $x$-polarized signal photon and a rotated $y$-polarized idler photon, then the output state referred to the two channels 1 and 2 illustrated in Fig. 1 is



© 1988 The American Physical Society

the linear superposition state[15,16]

$$|\psi\rangle=(T_xT_y)^{1/2}|1_{1x},1_{2y}\rangle+(R_xR_y)^{1/2}|1_{1y},1_{2x}\rangle-i(R_yT_x)^{1/2}|1_{1x},1_{1y}\rangle+i(R_xT_y)^{1/2}|1_{2x},1_{2y}\rangle. \quad (2)$$

Here $R_x,R_y,T_x,T_y$ are the beam-splitter reflectivities and transmissivities with $R_x+T_x=1=R_y+T_y$, and we have made use of the well-known Fresnel formulas for reflection and transmission amplitudes. For a symmetric beam splitter the phases of the reflected and transmitted waves always differ by $\pm\pi/2$. The polarized scalar fields $\hat{E}_1^{(+)}$ and $\hat{E}_2^{(+)}$ at the two detectors are related to the vector fields $\hat{\mathcal{E}}_1^{(+)}$ and $\hat{\mathcal{E}}_2^{(+)}$, respectively, after the beam splitter and before the polarizers by (Hilbert-space operators are labeled by the caret)

$$\hat{E}_1^{(+)}=\cos\theta_1\hat{\mathcal{E}}_{1x}^{(+)}+\sin\theta_1\hat{\mathcal{E}}_{1y}^{(+)},\quad \hat{E}_2^{(+)}=\cos\theta_2\hat{\mathcal{E}}_{2x}^{(+)}+\sin\theta_2\hat{\mathcal{E}}_{2y}^{(+)}. \quad (3)$$

The joint two-photon detection probability $P(\theta_1\theta_2)$ is then given by[17]

$$P(\theta_1,\theta_2)=K\langle\psi|\hat{E}_1^{(-)}\hat{E}_2^{(-)}\hat{E}_2^{(+)}\hat{E}_1^{(+)}|\psi\rangle, \quad (4)$$

where $K$ is characteristic of the detector efficiency. With the help of Eqs. (2) and (3) we readily obtain

$$P(\theta_1,\theta_2)=K[(T_xT_y)^{1/2}\cos\theta_1\sin\theta_2+(R_xR_y)^{1/2}\sin\theta_1\cos\theta_2]^2, \quad (5a)$$

which reduces to

$$P(\theta_1,\theta_2)=\tfrac{1}{4}K\sin^2(\theta_2+\theta_1)\ \text{ when }\ R_x=\tfrac{1}{2}=T_x,\ R_y=\tfrac{1}{2}=T_y. \quad (5b)$$

If the polarizer angles are chosen so that

$$\theta_1=\pi/8,\quad \theta_2=\pi/4,\quad \theta_1'=3\pi/8,\quad \theta_2'=0, \quad (6)$$

then one finds with the help of relations (1) and (5) for a 50%:50% beam splitter with $R_x=\frac{1}{2}=T_x$, $R_y=\frac{1}{2}=T_y$, that

$$S=\tfrac{1}{4}K(\sqrt{2}-1)>0, \quad (7)$$

so that the Bell inequality is violated. More generally, for any $T_x,T_y,R_x,R_y$,

$$S=\tfrac{1}{4}K[(-2+\sqrt{2})T_xT_y+(-2+\sqrt{2})R_xR_y+2\sqrt{2}(T_xT_yR_xR_y)^{1/2}]. \quad (8)$$

In practice $R_x/T_x$ and $R_y/T_y$ were both about 0.95 in the experiment.

Let us suppose that $\theta_2=\pi/4$. Then Eq. (5a) yields

$$\begin{aligned}P(\theta_1,\pi/4)&=\tfrac{1}{4}K[(T_xT_y+R_xR_y)+2(T_xT_yR_xR_y)^{1/2}\sin2\theta_1-(T_xT_y-R_xR_y)\cos2\theta_1]\\&=\tfrac{1}{4}K(T_xT_y+R_xR_y)[1+\sin(2\theta_1-\beta)],\end{aligned} \quad (9)$$

where

$$\beta=\arctan(T_xT_y-R_xR_y)/2(T_xT_yR_xR_y)^{1/2}. \quad (10)$$

In particular, when $R_x=\frac{1}{2}=T_x$, $R_y=\frac{1}{2}=T_y$,

$$P(\theta_1,\pi/4)=\tfrac{1}{8}K[1+\sin2\theta_1]. \quad (11)$$

Hence the joint probability $P(\theta_1,\pi/4)$ exhibits a sinusoidal modulation with respect to the angle $2\theta_1$, with 100% relative modulation. It is interesting to observe that if an attenuator, such as a neutral density filter NDF, were inserted in either the signal or idler beam as indicated by the dashed outline in Fig. 1, the joint probability $P(\theta_1,\pi/4)$ would be reduced, because the apparatus responds only to photon pairs, but the $\theta_1$ dependence given by Eq. (9) or (11) and the 100% relative modulation would be unchanged.

*Classical theory.*— Next we calculate the joint detection probability $P(\theta_1,\theta_2)$ by classical wave optics. Let $\mathbf{E}_s^{(+)},\mathbf{E}_i^{(+)}$ represent the complex signal and idler fields just before the beam splitter. Then, after taking into account the fact that the signal field is $x$ polarized and the idler field is $y$ polarized, we obtain for the complex fields $E_1^{(+)},E_2^{(+)}$ at the two detectors

$$E_1^{(+)}=\cos\theta_1\sqrt{T_x}E_s^{(+)}-i\sin\theta_1\sqrt{R_y}E_i^{(+)}, \quad (12)$$

$$E_2^{(+)}=i\cos\theta_2\sqrt{R_x}E_s^{(+)}+\sin\theta_2\sqrt{T_y}E_i^{(+)}. \quad (13)$$

Now the joint detection probability $P(\theta_1,\theta_2)$ is proportional to the intensity correlation $\langle|E_1^{(+)}|^2|E_2^{(+)}|^2\rangle$. On taking the phases of $E_s^{(+)}$ and $E_i^{(+)}$ to be random and uncorrelated on the grounds that signal and idler photons do not give rise to second-order interference effects, we readily find from Eqs. (12) and (13)

$$\begin{aligned}P(\theta_1,\theta_2)=C\{&\langle I_sI_i\rangle[(T_xT_y)^{1/2}\cos\theta_1\sin\theta_2+(R_xR_y)^{1/2}\sin\theta_1\cos\theta_2]^2\\&+\langle I_s^2\rangle R_xT_x\cos^2\theta_1\cos^2\theta_2+\langle I_i^2\rangle R_yT_y\sin^2\theta_1\sin^2\theta_2\},\end{aligned} \quad (14)$$

TABLE I. Results of coincidence counting measurements for certain combinations of polarizer angles $\theta_1$ and $\theta_2$.

| $\theta_1$ | $\theta_2$ | Coincidence rate per minute $\mathcal{R}$ |
|---|---|---|
| 67.5° | 45° | $28.3 \pm 0.8$ |
| 22.5° | 45° | $29.8 \pm 0.8$ |
| 67.5° | 0° | $29.9 \pm 0.8$ |
| 22.5° | 0° | $5.6 \pm 0.7$ |
| 67.5° | No polarizer | $34.7 \pm 0.9$ |
| No polarizer | 45° | $36.2 \pm 0.9$ |

where we have written $I_s = |E_s^{(+)}|^2$, $I_i = |E_i^{(+)}|^2$ for the signal and idler intensities. $C$ is a constant characteristic of the detector. Comparison with Eq. (5a) shows similarities, but the terms in $\langle I_s^2 \rangle$ and $\langle I_i^2 \rangle$ are absent in the quantum-mechanical case, because we are dealing with single signal and idler photons.

In the special case $R_x = \frac{1}{2} = T_x$, $R_y = \frac{1}{2} = T_y$, and when $\theta_2 = \pi/4$, Eq. (14) reduced to

$$P(\theta_1, \pi/4) = \tfrac{1}{16} C[\langle (I_s + I_i)^2 \rangle + \mathcal{A} \sin(2\theta_1 - \gamma)], \quad (15)$$

where

$$\mathcal{A} = [(\langle I_i^2 \rangle - \langle I_s^2 \rangle)^2 + 4\langle I_i I_s \rangle^2)^{1/2},$$
$$\gamma = \arctan [(\langle I_i^2 \rangle - \langle I_s^2 \rangle)/2\langle I_i I_s \rangle]. \quad (16)$$

If we make the simplifying assumptions about the intensity fluctuations that $\langle I_s^2 \rangle = \langle I_s \rangle^2 (1+\lambda)$, $\langle I_i^2 \rangle = \langle I_i \rangle^2 (1+\lambda)$, $\langle I_i I_s \rangle = \langle I_i \rangle \langle I_s \rangle (1+\lambda)$, then the relative modulation or "visibility" $\mathcal{V}$ in Eq. (15) becomes

$$\mathcal{V} = (\langle I_i \rangle^2 + \langle I_s \rangle^2)/(\langle I_i \rangle + \langle I_s \rangle)^2, \quad (17)$$

which is always less than unity and has the value $\frac{1}{2}$ when $\langle I_s \rangle = \langle I_i \rangle$. This is in contrast to the quantum-mechanical result embodied in Eq. (11). In the special case $\langle I_i \rangle = \langle I_s \rangle$, Eq. (15) reduces to

$$P(\theta_1, \pi/4) = \tfrac{1}{4} C \langle I_s \rangle^2 [1 + \tfrac{1}{2} \sin 2\theta_1]. \quad (18)$$

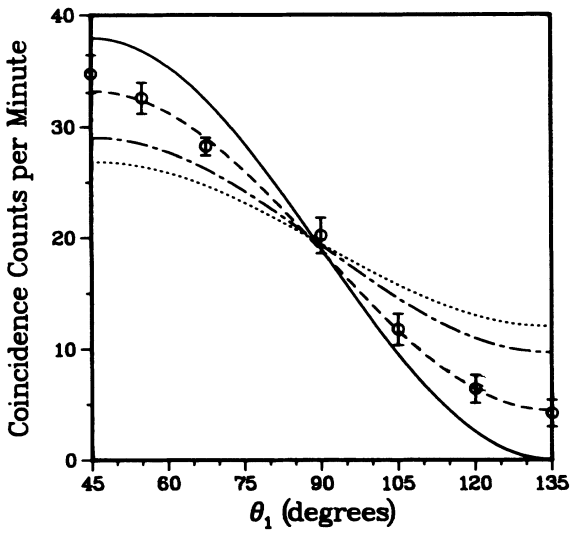


FIG. 2. Measured coincidence counting rate as a function of the polarizer angle $\theta_1$, with $\theta_2$ fixed at 45°. The full curve is the quantum prediction based on Eq. (11) and the dash-dotted curve is the classical prediction based on Eq. (18). The dashed and dotted curves are obtained by multiplication of the sinusoidal functions in Eqs. (11) and (18), respectively, by 0.76 to allow for reduced modulation caused by imperfect alignment.

From Eq. (16) the phase $\gamma$ of the modulation depends on the intensity ratio $\langle I_s \rangle / \langle I_i \rangle = R$. Although $\gamma = 0$ when $R = 1$, for very small or very large $R$ the phase $\gamma$ tends towards $\pm \pi/2$. This is again in contrast to the quantum-mechanical result given by Eq. (11), for which the phase of the modulation is independent of the ratio of signal to idler photons.

Table I shows the results of coincidence counting measurements for certain combinations $\theta_1, \theta_2$ of the polarizer angles, and after subtraction of accidentals. As the coincidence rate is proportional to $P(\theta_1, \theta_2)$, we can calculate the combination $S$ given by relation (1) up to a scale constant. If $\tilde{S}$ is the quantity analogous to $S$ but expressed in terms of the coincidence rates, we find

$$\tilde{S} = \mathcal{R}(22.5°, 45°) - \mathcal{R}(22.5°, 0°) + \mathcal{R}(67.5°, 45°) + \mathcal{R}(67.5°, 0°) - \mathcal{R}(67.5°, -) - \mathcal{R}(-, 45°)$$
$$= (11.5 \pm 2.0)/\text{min}. \quad (19)$$

Hence $\tilde{S}$ is positive with an accuracy of about 6 standard deviations, in violation of the Bell inequality (1). Unlike Alley and Shih,[9] we prefer to base our conclusions on the quantity $\tilde{S}$ rather than on their simpler counting-rate ratio $\delta$, because the Bell inequality (1) does not depend on symmetry with respect to $\theta_1, \theta_2$, and the threshold for violation occurs at $\tilde{S} = 0$.

When $\theta_2$ is fixed at 45° and the angle $\theta_1$ is varied, the results of the coincidence counting measurements are illustrated in Fig. 2. The solid curve and the dash-dotted curve in Fig. 2 correspond to the quantum-mechanical prediction given by Eq. (11) and the classical wave prediction given by Eq. (18), respectively, with the scale constants $K$ and $C$ adjusted for best fit. The mean counting rates of detectors 1 and 2 were 2600/sec and 2800/sec when $\theta_1 = \theta_2 = 45°$. It will be seen that $P(\theta_1, \pi/4)$ does indeed exhibit the expected sinusoidal modulation with the angle $\theta_1$, with half period of 90°. The observed relative modulation $\mathcal{V}$ obtained from the best fitting curve is about 0.76, which is greater than the 0.50 figure predicted by the classical relation (18), but below the 100% value given by the quantum relation (11). We believe that the reason for the observed depth

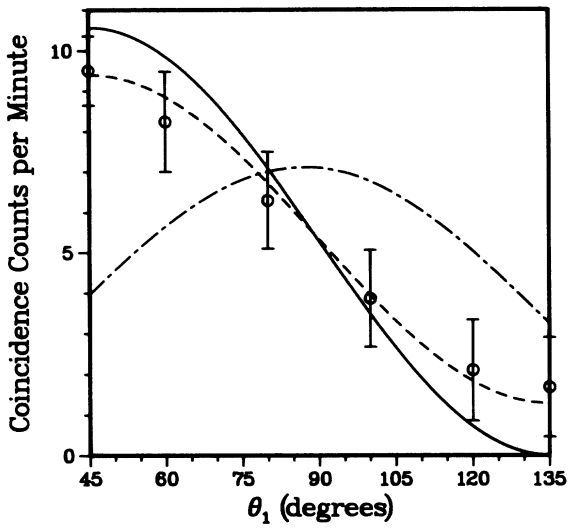


FIG. 3. Measured coincidence counting rate as a function of the polarizer angle $\theta_1$, with $\theta_2$ fixed at 45°, when an 8:1 attenuator is inserted into the idler beam. The full curve is the quantum prediction based on Eq. (11) and the dash-dotted curve is the classical prediction based on Eq. (15). The dashed curve is obtained by multiplication of the sinusoidal function in Eq. (11) by 0.76 to allow for reduced modulation caused by imperfect alignment.

of modulation falling below 100% is imperfection in the alignment of signal and idler waves; similar alignment problems led to reduced visibility in a previous experiment.[11] A more detailed theory that allows corrections for the size of the detector aperture and possible misalignment to be made leads to a relative modulation below 100%.[16] The dashed and dotted curves in Fig. 2 were obtained by multiplication of the sinusoidal terms in Eqs. (11) and (18), respectively, by the factor 0.76 to allow for these effects.

When an 8:1 neutral density filter NDF is inserted in the path of the idler photons, and a compensating, nonabsorbing glass plate $C_2$ in the path of the signal photons, as indicated in Fig. 1, we obtain the results shown in Fig. 3. Once again, the solid curve and the dash-dotted curve are based on the corresponding quantum and classical predictions given by Eqs. (11) and (15), respectively, with the scale constants adjusted for best fit. Because the attenuator results in a greatly reduced coincidence counting rate, the statistical uncertainties of the experimental points are much larger than before. Nevertheless, it is clear that the observed $\theta_1$ dependence is virtually unchanged, as predicted by the quantum calculation, and quite different from the classical form when $\langle I_i\rangle/\langle I_s\rangle = \frac{1}{8}$. The dashed curve in Fig. 3 is obtained when the sinusoidal term in Eq. (11) is again multiplied by 0.76, to allow for reduced visibility attributable to imperfect alignment.

We have therefore demonstrated that the observed counting rates in the correlation experiment violate both Einstein locality, expressed by the Bell inequality, for particles and the classical probability relations for waves.

This work was supported by the National Science Foundation and by the U.S. Office of Naval Research.

[1]C. S. Wu and I. Shaknov, Phys. Rev. **77**, 136 (1950).

[2]C. A. Kocher and E. D. Commins, Phys. Rev. Lett. **18**, 575 (1967).

[3]S. J. Freedman and J. F. Clauser, Phys. Rev. Lett. **28**, 938 (1972).

[4]J. F. Clauser, Phys. Rev. Lett. **36**, 1223 (1976).

[5]E. S. Fry and R. C. Thompson, Phys. Rev. Lett. **37**, 465 (1976).

[6]A. Aspect, P. Grangier, and G. Roger, Phys. Rev. Lett. **47**, 460 (1981), and **49**, 91 (1982).

[7]A. Aspect, J. Dalibard, and G. Roger, Phys. Rev. Lett. **49**, 1804 (1982).

[8]A. J. Duncan, W. Perrie, H. J. Beyer, and H. Kleinpoppen, in *Fundamental Processes in Atomic Collision Physics,* edited by H. Kleinpoppen *et al.,* NATO Advanced Studies Institute, Ser. B, Vol. 134 (Plenum, New York, 1985), p. 555.

[9]C. O. Alley and Y. H. Shih, in Proceedings of the Fifteenth International Quantum Electronics Conference, Baltimore, Maryland, 1987 (to be published), paper No. TU003, and in *Proceedings of the Second International Symposium on Foundations of Quantum Mechanics in the Light of New Technology, Tokyo, 1986,* edited by M. Namiki *et al.* (Physical Society of Japan, Tokyo, 1987).

[10]R. Ghosh and L. Mandel, Phys. Rev. Lett. **59**, 1903 (1987).

[11]C. K. Hong, Z. Y. Ou, and L. Mandel, Phys. Rev. Lett. **59**, 2044 (1987).

[12]J. F. Clauser and M. A. Horne, Phys. Rev. D **10**, 526 (1974).

[13]J. S. Bell, Physics (Long Island City, N.Y.) **1**, 195 (1964).

[14]J. F. Clauser and A. Shimony, Rep. Prog. Phys. **41**, 1881 (1978).

[15]Z. Y. Ou, C. K. Hong, and L. Mandel, Opt. Commun. **63**, 118 (1987).

[16]Z. Y. Ou, Phys. Rev. A **37**, 1607 (1988).

[17]R. J. Glauber, Phys. Rev. **130**, 2529 (1963), and **131**, 2766 (1963).

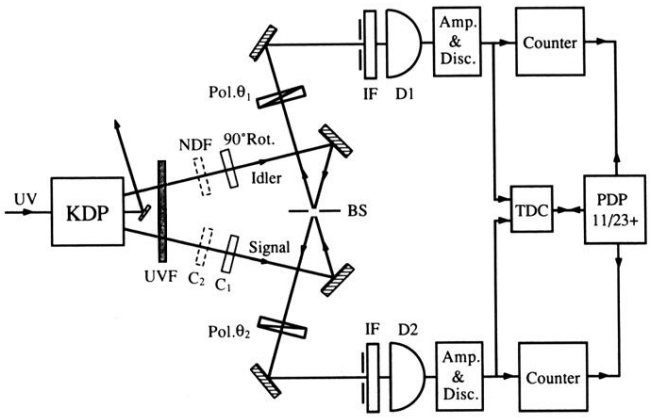


FIG. 1. Outline of the apparatus.